Title
Components of Particle Emissions from Light-Duty Spark-Ignition Vehicles with Varying Aromatic Content and Octane Rating in Gasoline

Journal
Environmental Science & Technology, 49(17)

ISSN
0013-936X 1520-5851

Authors
Short, Daniel Z
Vu, Diep
Durbin, Thomas D
et al.

Publication Date
2015-08-17

DOI
10.1021/acs.est.5b03138

Peer reviewed

Environmental Science & Technology

Article

pubs.acs.org/est

Components of Particle Emissions from Light-Duty Spark-Ignition Vehicles with Varying Aromatic Content and Octane Rating in Gasoline

Daniel Z. Short,[†,‡] Diep Vu,[†,‡] Thomas D. Durbin,[†,‡] Georgios Karavalakis,[†,‡] and Akua Asa-Awuku*[,†,‡]

[†]Department of Chemical and Environmental Engineering, University of California- Riverside, 900 University Ave., Riverside 92507, California, United States

[‡]College of Engineering- Center for Environmental Research and Technology, University of California- Riverside, 1084 Columbia Ave., Riverside 92521, California, United States

Supporting Information

ABSTRACT: Typical gasoline consists of varying concentrations of aromatic hydrocarbons and octane ratings. However, their impacts on particulate matter (PM) such as black carbon (BC) and water-soluble and insoluble particle compositions are not well-defined. This study tests seven 2012 model year vehicles, which include one port fuel injection (PFI) configured hybrid vehicle, one PFI vehicle, and six gasoline direct injection (GDI) vehicles. Each vehicle was driven on the Unified transient testing cycle (UC) using four different fuels. Three fuels had a constant octane rating of 87 with varied aromatic concentrations at 15%, 25%, and 35%. A fourth fuel with higher octane rating, 91, contained 35% aromatics. BC, PM mass, surface tension, and water-soluble organic mass (WSOM) fractions were measured. The water-insoluble mass (WIM) fraction of the vehicle emissions was estimated. Increasing fuel aromatic content increases BC emission factors (EFs) of transient cycles. BC concentrations were higher for the GDI vehicles than the PFI and hybrid vehicles, suggesting a potential climate impact for increased GDI vehicle production. Vehicle steady-state testing showed that the hygroscopicity of PM emissions at high speeds (70 mph; $\kappa > 1$) are much larger than emissions at low speeds (30 mph; $\kappa < 0.1$). Iso-paraffin content in the fuels was correlated to the decrease in WSOM emissions. Both aromatic content and vehicle speed increase the amount of hygroscopic material found in particle emissions.

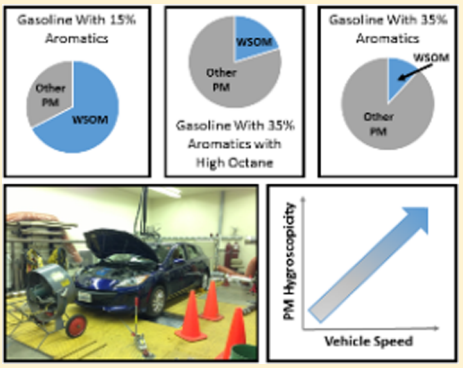

INTRODUCTION

Gasoline manufactured in the U.S. contains several components (e.g., oxygenates and aromatic compounds) that are used to modify gasoline octane rating. For example, tetraethyl lead (TEL), was used to increase the octane rating, and improved combustion.[1] However, TEL proved to be detrimental to air quality and was banned from all consumer fuels.[1] Other octane boosting blending components were found to replace TEL including oxygenates, such as ethanol, and aromatic hydrocarbons.[1−3] Different combinations of compounds are used to modulate octane ratings and the regulations of these additives in the U.S. are enforced by state and federal governments. For example, the California Air Resources Board (CARB) limits the amount of aromatic hydrocarbons to be 35% by volume in gasoline.[4] The federal average level for aromatic hydrocarbons for conventional gasoline in the U.S. is ∼29% for summer and winter blends.[5] Gasoline blends with 10% ethanol are found in most gas stations across the U.S.[6] However, due to the increased ethanol concentration in fuels over the past decade, manufacturers have reduced the aromatic content in gasoline to maintain a reasonable octane rating.[7] If this trend continues, aromatic concentrations could be considerably lower if ethanol concentrations increase.

In the U.S, conventional vehicle technologies consume commercial gasoline fuels of varying aromatic content and octane rating. Gasoline engines equipped with port fuel injection (PFI) systems currently dominate the light-duty vehicle market in the U.S.[8] In PFI systems, the fuel is injected on the backside of the intake valves to take advantage of warm valves and port surfaces to help vaporize the fuel spray. Hybrid vehicles use a variation of PFI engine technology and an electric motor alternately to decrease fuel usage and increase the rate of energy storage. On the other hand, gasoline direct injection (GDI) engines are becoming more prevalent, and are predicted to dominate the U.S. market in the future.[8,9] Unlike PFI operation, in GDI engines the fuel is injected directly into the combustion chamber.[8] The advantage of the GDI injection strategy is that it improves engine efficiency and fuel economy.

Received: August 11, 2014
Revised: August 3, 2015
Accepted: August 5, 2015
Published: August 5, 2015

DOI: 10.1021/acs.est.5b03138
Environ. Sci. Technol. 2015, 49, 10682−10691

Previous studies have shown higher particulate matter (PM) emissions with GDI engines compared to PFI engines. Fuel impingement on the piston and cylinder surfaces (pool fires) in GDI engines can generate liquid fuel that is partially vaporized and not well mixed with ambient air at the start of combustion, leading to charge heterogeneity and localized fuel-rich regions in the charge cloud and higher PM concentrations.[10,11]

Increased vehicular particle emissions can cause adverse health effects.[12−14] Specific components of vehicle PM composition, such as water-soluble components, can pose a health risk to humans (refs 12−16 and references therein). For example, water-soluble PM has been linked to pulmonary and cardiovascular diseases, and long-term exposure is known to cause human DNA damage.[12,13] In addition, water-soluble PM has been linked with the cellular production of reactive oxygen species (ROS).[16−18] Furthermore, water-soluble nanoparticles can grow to micron droplet sizes when inhaled leading to increased PM deposition rates.[19] Variation in water-soluble emissions can affect aerosol hygroscopicity and cloud condensation nuclei (CCN) activity thus impacting visibility and climate.[20] Thus, the amount of hygroscopic and water-soluble aerosol from vehicle emissions must be measured to assess potential impacts on climate and human health.

To our knowledge, there is a dearth of information on the particle number and composition from the emissions of combusted fuels specifically blended to vary aromatic concentrations and octane ratings. There exist numerous studies that lower the aromatic concentration by the addition of ethanol to the fuel. Many of these studies have shown that the addition of ethanol, which lowered the total aromatic content of the fuel, and decreased the PM emissions.[21,22] However, Chen et al.[23] showed that the addition of ethanol in gasoline led to an increase in PM emissions. It is important to note that the gasoline used in Chen et al.[23] had a relatively high iso-paraffin concentration compared to studies that added ethanol to reduced aromatic concentrations. The primary focus of this work is to determine particle hygroscopicity and composition for emissions from current light-duty vehicles (LDVs). This paper presents changes in PM emissions for different fuels, engine technologies, and operating conditions. Specifically, we characterize the effect on PM of decreased aromatic content fuels combusted in advanced vehicle technologies. PM mass and particle number (PN) emissions were found to be higher for the GDI vehicles compared to their PFI counterparts, as shown in a companion paper to this study.[24] Data presented here shows vehicle speed effects on BC emissions rates and water-insoluble particle composition from fuels with varying aromatic content and octane ratings. A companion paper to this study presents the criteria pollutant and air toxic emissions associated with this study.[24]

EXPERIMENTAL METHODS

Testing Procedure. Vehicles were tested at the vehicle emissions research laboratory (VERL) located at the College of Engineeing-Center for Environmental Research and Tehcnology (CE-CERT). VERL is equipped with a Burke E. Porter light-duty chassis dynamometer and a constant volume sampler (CVS) that creates uniform dilution of the emissions from the tailpipe for each vehicle. Vehicles were tested over three different unified cycle (UC) tests. Additional information about this transient cycle can be found in the Supporting Information (SI) 1.1 and the speed trace plot of the UC is shown in Figure S1. In addition, at the end of each UC test, steady-state cycles at 30 mph, 50 mph, and 70 mph were conducted for each vehicle/fuel combination.

Test Vehicles and Fuels. A total of seven vehicles were tested, including five passenger cars and two light-duty trucks. The vehicle engine configurations included five wall-guided, stoichiometrically operated GDI vehicles, one hybrid vehicle with PFI fueling, and one conventional PFI vehicle. These vehicles are listed in Table S1. All vehicles, with the excpetion of one, were certified to meet the Federal Tier 2, Bin 2 exhaust emission standards or the California LEV-II, SULEV exhaust emissions standards. Although Tier-3 regulations have yet to be implemented, these vehicles are reasonably representative of vehicles that would be seen under Tier 3 regulations, and as such are termed Tier 3 like. The Ford F-150 was certified to meet the Tier 2 Bin 4 emission certification.

Four fuels with varying aromatic content were used in this study. The fuels were blended with nominal aromatic contents of 15%, 25%, and 35% by volume. In addition, a fourth fuel was used that had a higher octane number, but the same aromatic content as the third fuel (35% aromatics by volume) with the higher octane from increased iso-paraffins. These aromatic fuels were blended to be within 0.5 vol % of the specific aromatic target. Sulfur content was maintained at ∼27 ppm. All fuels were blended with ∼10 vol % ethanol (E10). The lubrication oil used was 5W-20 and nonsynthetic. Additional fuel properties are listed in Table S2.

Online Particle Water-Insolubility. A schematic of the instrumentation setup for all the instruments used in this study is shown in Figure S2. For the experimental setup, a water-condensation particle counter (W-CPC) (TSI model 3785) and butanol-CPC (B-CPC) (TSI model 3772) were used with an electrostatic classifier (TSI model 3080). A scanning mobility particle sizer (SMPS) determined the size and number of particles.[25] The characterization of the size distribution is important, as heterogeneous particle nucleation is a function of particle size. The electrostatic classifier selects a particle diameter between 10 and 289 nm, and the dry particles exiting the classifier are split into streams going to the B-CPC and the W-CPC. A particle scan from 10 to 280 nm takes approximately 135 seconds; ∼17 scans were completed during a UC. Previous studies have shown significant differences between butanol and water-based CPCs for particles below 40 nm.[26] The difference is due to the particle hygroscopicity properties or κ. As the surface area of the particle decreases, the probability of droplet activation depends increasingly on its hygroscopicity.[27] In addition, as κ approaches 1, the particles are more hygroscopic and more water-soluble; as κ approaches 0, particles are less hygroscopic and likely less water-soluble.

Figure S3 shows the real-time plot of the ratio of water to butanol particle counts for a given SMPS scan. The plot shows a sigmoidal distribution from 0 to 1. When the ratio = 0.5, 50% of the total particles form droplets within the W-CPC. The diameter of the particles at this 50% threshold is known as the critical diameter, or d_s. The operation is under the assumption that the B-CPC provides total particle number. The diameter, d_s, that corresponds to this 0.5 ratio is used to estimate the water-insoluble mass (WIM) fraction. The WIM fraction is the total fraction of particles that exhibit water-insoluble properties for particles with diameters below 40 nm. The method is calibrated with aerosolized ammonium sulfate. The d_s for ammonium sulfate was 20.5 nm for the W-CPC instrument critical supersaturation, and is consistent with previously published results.[28] To find a cumulative overall WIM fraction

DOI: 10.1021/acs.est.5b03138
Environ. Sci. Technol. 2015, 49, 10682−10691

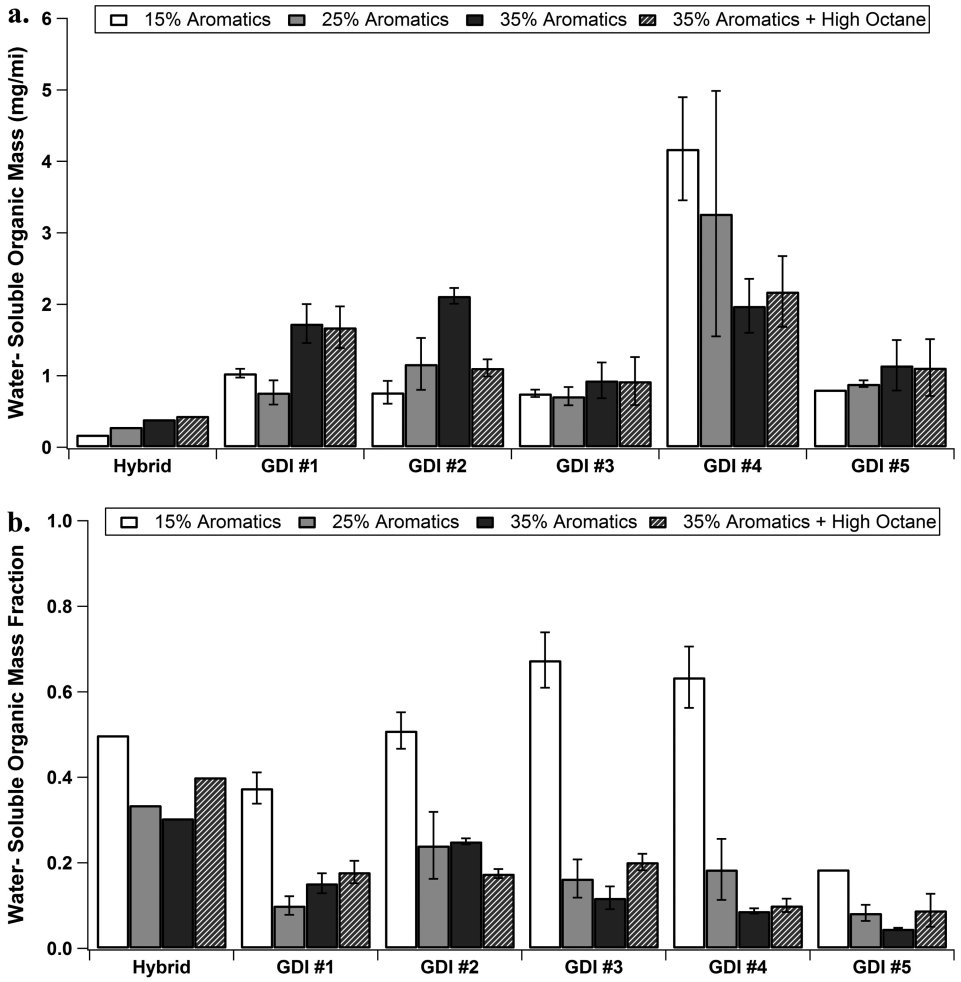

Figure 1. WSOM Emission Factor (a.) and the WSOM/PM mass Fraction (b.) over the unified cycle for six vehicles tested.

over a driving cycle, the total W-CPC to B-CPC ratio was calculated. The ratio was calculated by the sum of each total particle number for every particle diameter selected by the electrostatic classifier. A plot of the ratio was used to determine an overall d_s for a particular vehicle and fuel. Supplemental Section 2 and Short et al.[26] give a more detailed description of the method to determine the WIM fraction from d_s. This method for determining the WIM fraction has been previously applied to vehicle tailpipe emissions in Short et al.,[29] and a more detailed description of the method is also provided.

Water-Soluble Organic Mass Fraction and Surface Tension Measurement. Teflon filter samples were collected during each UC test to determine the WSOC concentrations and particle surface tension. Hence, the WSOC and surface tension measurements are representative of the cumulative aerosol composition. Each filter was placed in a vial and sonicated for 90 min with Millipore DI water (18 mΩ, < 100 ppb). Once sonicated, large nondissolved particles were removed using a Whatman 25 mm syringe filter. The sample was then diluted into ratios of 1:1, 1:3, and 1:5. The surface tension, σ_b, for each samples was measured with a pendant drop tensiometer (Attension Theta 200). The tensiometer fits the droplet image to the Young−Laplace equation to compute the droplet surface tension. 100 images were captured for each droplet. The WSOC concentrations of these samples were measured using a GE Sievers 900 total organic carbon (TOC) analyzer. The instrument measures the total dissolved organic carbon and inorganic carbon. The total dissolved organic carbon concentration, in ppm or mg/L, was then multiplied by the amount of water added (60 mL). The WSOC concentration was then multiplied by the ratio of the average organic molecular weight per carbon weight, 1.2, to account for all water-soluble organic noncarbonaceous components.[30] This term is defined as the water-soluble organic mass (WSOM). The WSOM mass was divided by the total mass of PM on the filter to determine the water-soluble organic mass fraction.

Online Black Carbon Measurement. A multi-angle absorption photometer (MAAP) (Thermo Scientific model 5012) was used to measure BC concentrations. The MAAP applies a light source at ∼670 nm on a flat layer of aerosol accumulated on Teflocarbon filter paper. Four optical detectors, above the filter paper, then determine the backscattering of light from the aerosol. The scattering is correlated with the concentration of black carbon. The instrument is calibrated two ways. The thermometer, pressure sensor, and sample flow rate are calibrated first. The calibration is verified by aerosolizing Aquadag© BC solution and simultaneously measuring the solution with an aerosol particle mass (APM, Kanomax model 3600) analyzer and the MAAP.[31] The calibrations used in this test resulted in agreement within ±12% for the APM measurements.

DOI: 10.1021/acs.est.5b03138
Environ. Sci. Technol. 2015, 49, 10682−10691

Table 1. Paraffin and Isoparaffin Compounds in All Fuels with WSOC/PM Mass Fraction Emissions for Six Vehicles Tested

	total paraffins (wt %)	total isoparaffins (wt %)	C8 isoparaffins (wt %)	2,2,4-trimethylpentane (wt %)	hybrid (WSOM/PM)	GDI #1 (WSOM/PM)	GDI #2 (WSOM/PM)	GDI #3 (WSOM/PM)	GDI #4 (WSOM/PM)	GDI #5 (WSOM/PM)
15% aromatics	9.21	40.69	20.54	13.70	0.498	0.375	0.509	0.674	0.634	0.185
25% aromatics	12.93	26.39	10.87	6.55	0.335	0.100	0.241	0.163	0.184	0.083
35% aromatics	13.17	20.2	3.62	2.49	0.304	0.152	0.250	0.118	0.087	0.046
35% aromatics with High octane	12.08	23.87	10.9	9.31	0.4	0.178	0.175	0.202	0.101	0.089

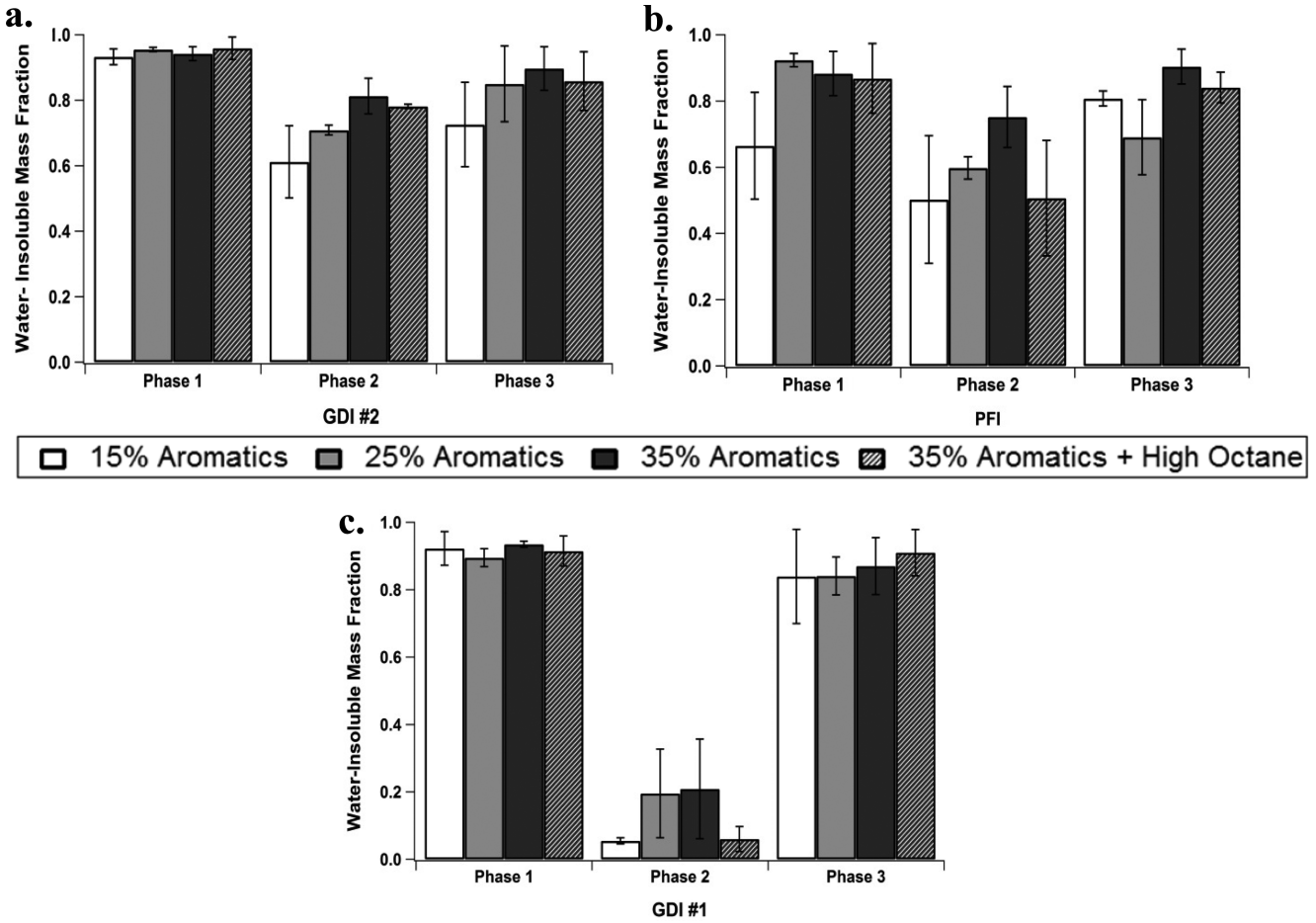

Figure 2. Water-insoluble mass faction by Phase for the GDI #2 (a.), PFI (b.), and the GDI #1 (c.) computed over the unified cycle.

RESULTS AND DISCUSSION

Water-Soluble Organic Mass. Results are shown for six vehicles (excluding the PFI) and all four fuels over the UC in Figure 1a. The data represent the average of three trials with the error bars being the standard deviation of those trials. Consistent fuel trends are shown. WSOM emission factors increased with increasing aromatics. The average WSOM emission factor (EF) was 1.34 mg mi^{-1}. The GDI #4 showed the highest WSOM EF value and was 4.97 mg mi^{-1} for the 15% aromatic fuel. The WSOM EF for the hybrid increased by 37% from 0.29 mg mi^{-1} to 0.39 mg mi^{-1} for the 15% aromatic fuel compared to the 35% aromatic fuel. GDI #1 showed a 46% increase in the WSOM emission factor from 1.19 mg mi^{-1} for the 15% aromatic fuel to 1.73 mg mi^{-1} for the 35% aromatic fuel. GDI #5 had a WSOM EF increase of 42% from the 15% aromatic fuel to the 35% aromatic fuel. All three of these vehicles did not show a change in the WSOM EFs with an increase in the fuel octane rating. GDI #2 showed a 123% increase in the WSOM emission factor from the 15% to the 35% aromatic fuel. The increased octane rating fuel decreased the WSOM emission factor 47% to 1.1 mg mi^{-1} for GDI #2. For the GDI #3, the WSOM emission factor did not show an effect from the different aromatic contents or octane ratings with an average WSOM EF of 0.91 mg mi^{-1}.

In Figure 1b, the WSOM/PM mass fractions are shown for the six vehicles tested over the UC cycle. The 15% aromatic fuel had a consistently larger WSOM/PM mass fraction compared to the other fuels tested, ranging from 0.2 to 0.65. The other fuels range from 0.05 to 0.4 for the 15% aromatic fuel. The majority of the PM emissions were WSOM for the GDI #2, GDI #3, and the GDI #4. GDI #5 emitted the lowest WSOM/PM mass fractions of all the vehicles. The hybrid had a large fraction of WSOM for all fuels. The highest aromatic content fuels and the high octane rating fuel emitted WSOM

DOI: 10.1021/acs.est.5b03138
Environ. Sci. Technol. 2015, 49, 10682−10691

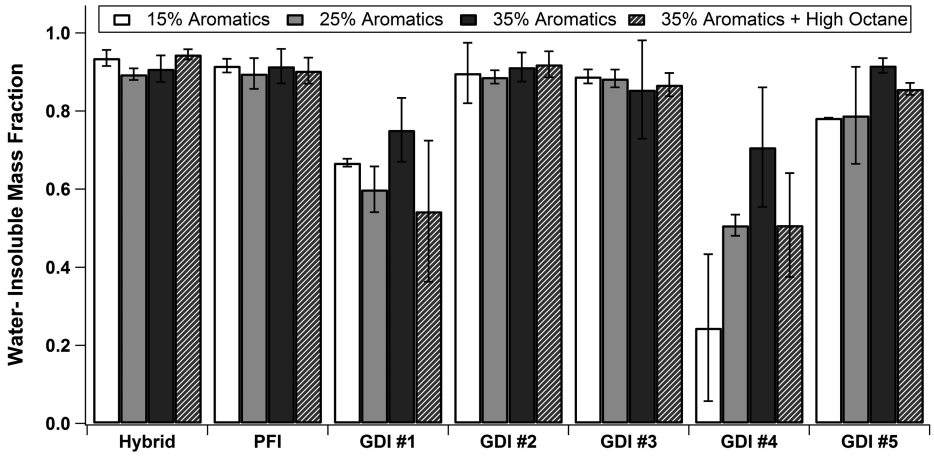

Figure 3. Water-insoluble mass faction calculated over the unified cycle.

(~0.15) emission factors similar to those reported in a previous study for a PFI vehicle.[32]

Paraffin and Isoparaffin Compound effects on WSOM/PM Mass Emissions. The WSOM/PM mass emissions were above a 0.40 fraction for the 15% aromatic fuel and were very low or below a 0.40 fraction for the other fuels. This trend was compared with several fuel compounds and a correlation was found between WSOM/PM mass fraction and iso-paraffins concentration, particularly with the dominate iso-parrafin compound of 2,2,4-trimethylpentane (iso-octane), in Table 1. The sum of the total isoparaffins, C_8 iso-paraffins, iso-octane were the highest of all paraffin compounds in the 15% aromatic fuel and dropped by half for the 25% aromatic fuel. The WSOC/PM mass fraction from 15% and 25% aromatic fuels decreased by 50%. The iso-paraffin amounts and WSOM/PM mass fractions for the other three fuels were relatively low (<10 wt % and <0.2).

Studies have shown that the oxidation of paraffins is possible with a three way catalyst (TWC).[33,34] In addition, Curran et al.[35] proposed mechanisms of iso-octane oxidation from which other carbon chain free radicals may form. Thus, the TWC could be potentially oxidizing these particular iso-paraffins, making the particles more soluble. The detailed organic composition is unavailable. However, it is possible that the oxidation of C_8 iso-paraffins would cause an increase in WSOM when an increased C_8 iso-paraffin concentration exists in the fuel.

The results suggest that increases in iso-paraffin concentration in the fuel increase WSOM. A 50% increase in iso-paraffin fuel concentrations increased the amount of WSOM emitted by as much as 50%. The inhalation of increased amounts of WSOM has been shown to impact human health[12−19]. In addition, communities near busy roadways with large concentrations of vehicular traffic could be especially vulnerable from increased WSOM emissions. Furthermore, increases in hygroscopic and WSOM emissions may impact cloud condensation nuclei (CCN) activity.[36] Increases in CCN number will impact climate by reflecting sunlight back into space, thus causing a cooling effect on the earth's surface.[37,38] Effectively quantifying vehicle EFs of WSOM and other water-soluble material could be crucial to obtaining a better radiative budget.

Water-Insoluble Mass Fraction by Phase. Figure 2 shows the results of the WIM faction for each individual phase of the UC. The data are the average of each trials respective phase with the error bars being the standard deviation of those trials. Collectively, the results suggest that particle emissions during phase 2 dictate the water-insolubility of the particles overall. Phase 2 was more transient in nature with higher average vehicle speed and load than cold-start and hot-start phases. The WIM fraction changed with respect to vehicle speed. The results from GDI #1, presented in Figure 2c, showed a more significant decrease in the WIM fraction between phases 1 and 2. Phase 1 and 3 PM emissions were largely water-insoluble, but phase 2 PM emissions were more soluble particle emissions. The WIM fraction for the 15% aromatic fuel decreased by 94% from phase 1 to phase 2, ranging from 0.05 to 0.9. Figure 2a shows the results from GDI #2 and Figure 2b shows the results from the PFI. These vehicles were selected because their water-insoluble particle emissions were representative of other vehicles in the fleet. For example, the PFI had similar water-insoluble particle emissions compared to the hybrid and the GDI #2 had water-insoluble particle emissions similar to those for the GDI #3 and GDI #5. In Figure 2a for the GDI #2, the WIM fraction for the 25% aromatic fuel decreased by 20% between phases 1 and 2. For the same fuel, the WIM fraction decreased by 35% for the PFI (Figure 2b), ranging from 0.59 to 0.91. The results from these two graphs show that phase 1 and 3 had higher WIM fractions compared to Phase 2. The results for the GDI #4, GDI #3, hybrid, and GDI #5 are shown in Figure S4.

Cumulative Water-Insoluble Mass Fraction. As shown in Figure 3, the majority of the cumulative emissions for the vehicles were water-insoluble. The hybrid, PFI, GDI #2, and GDI #3 do not show any particular fuel trends, with WIM fractions ~0.9. The GDI #1, GDI #4, and GDI #5 show increasing WIM fractions with increasing aromatic content. The WIM fractions for the GDI #1 increased by 23% between the 25% and 35% aromatic fuels, ranging from 0.59 to 0.76. GDI #1 showed that the highest octane rating fuel produced the lowest WIM fraction (0.54) of all four fuels. The other two vehicles showed an increase between the 15% and 35% aromatic content fuel of 189% for the GDI #4 and 17% for the GDI #5. For the GDI #4, the higher octane rating fuel showed an equivalent WIM fraction with the 25% aromatic content fuel (WIM fraction of 0.51). GDI #5 showed a 6% decrease in the WIM fraction from the 35% aromatic fuel to the high octane rating fuel.

Particle Hygroscopicity and BC Concentration during Vehicle Steady-State Speeds. The vehicles were driven at

DOI: 10.1021/acs.est.5b03138
Environ. Sci. Technol. 2015, 49, 10682−10691

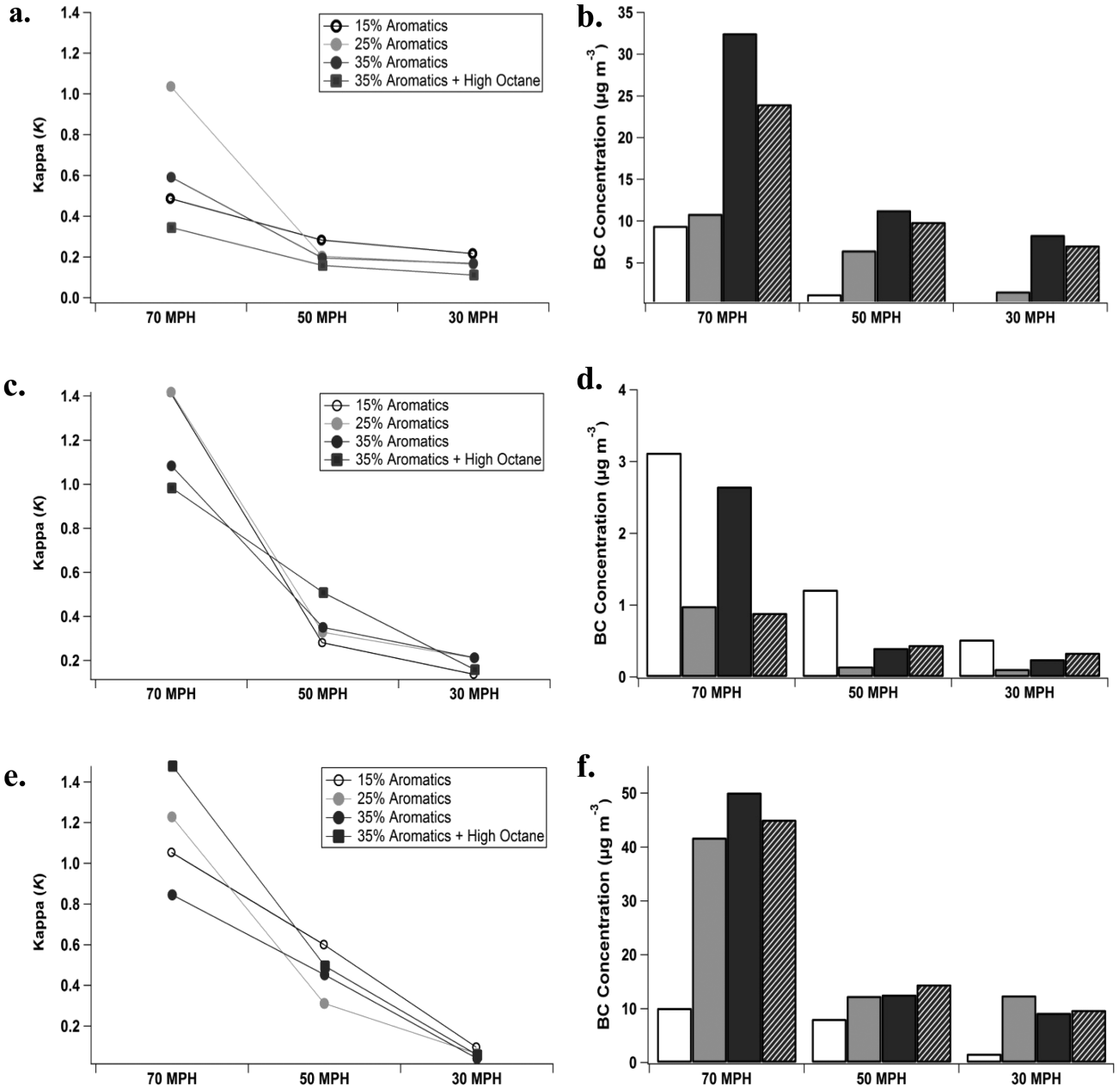

Figure 4. κ values for the GDI #2 (a.), PFI (c.), and GDI #1 (e.) and BC concentration for the GDI #2 (b.), PFI (d.), and the GDI #1 (f.) for steady-state vehicle speeds of 70, 50, 30 mph.

three different steady-state speeds of 70, 50, and 30 mph. To better understand particle water-insolubility during steady-state speeds the hygroscopicity term, κ, is reported. Particle hygroscopcity was calculated with Eq 3 provided in the SI. As stated in the experimental section, as κ approaches 1, the particles are more hygroscopic and likely less water-insoluble; as κ approaches 0, particles are less hygroscopic and likely more water-insoluble. The hygroscopicity of particles may exceed 1, such as the case of highly soluble salts (e.g., but not limited to NaCl and lithium salts). The results for the particle hygroscopicity values and BC concentrations for each steady-state condition are shown in Figure 4 for the GDI #1, GDI #2, and the PFI. These vehicles were chosen because of the similar WIM fraction results described in the Cumulative Water-Insoluble Mass Fraction section. The other vehicle steady-state results are shown in SI Figure S5. Some fuels during the 70 mph steady-state speed had κ values higher than 1, indicating the particles were highly hygroscopic. Sulfuric acid, a common vehicular emission component, has a κ value of 0.9.[29] It is important to note that some studies have reported a lower κ value for sulfuric acid, ranging between 0.68 and 0.74, but this study refers to the upper κ value reported for sulfuric acid of 0.9.[29,39] This suggests for $\kappa > 1$ that other highly hygroscopic components could be present in the emissions, but the specific components were not determined in this study. The majority of particle emissions at 70 mph tend to be less hydrophobic and water-insoluble.

The κ values for the GDI #1, GDI #2, and PFI vehicles over the steady-state cycles are shown in Figure 4a, 4c, and 4e, respectively. All vehicles show decreasing particle hygroscopicity with decreasing vehicle speed. For the GDI #2, the largest κ value was 1.05 for the 70 mph speed. The PFI showed

DOI: 10.1021/acs.est.5b03138
Environ. Sci. Technol. 2015, 49, 10682−10691

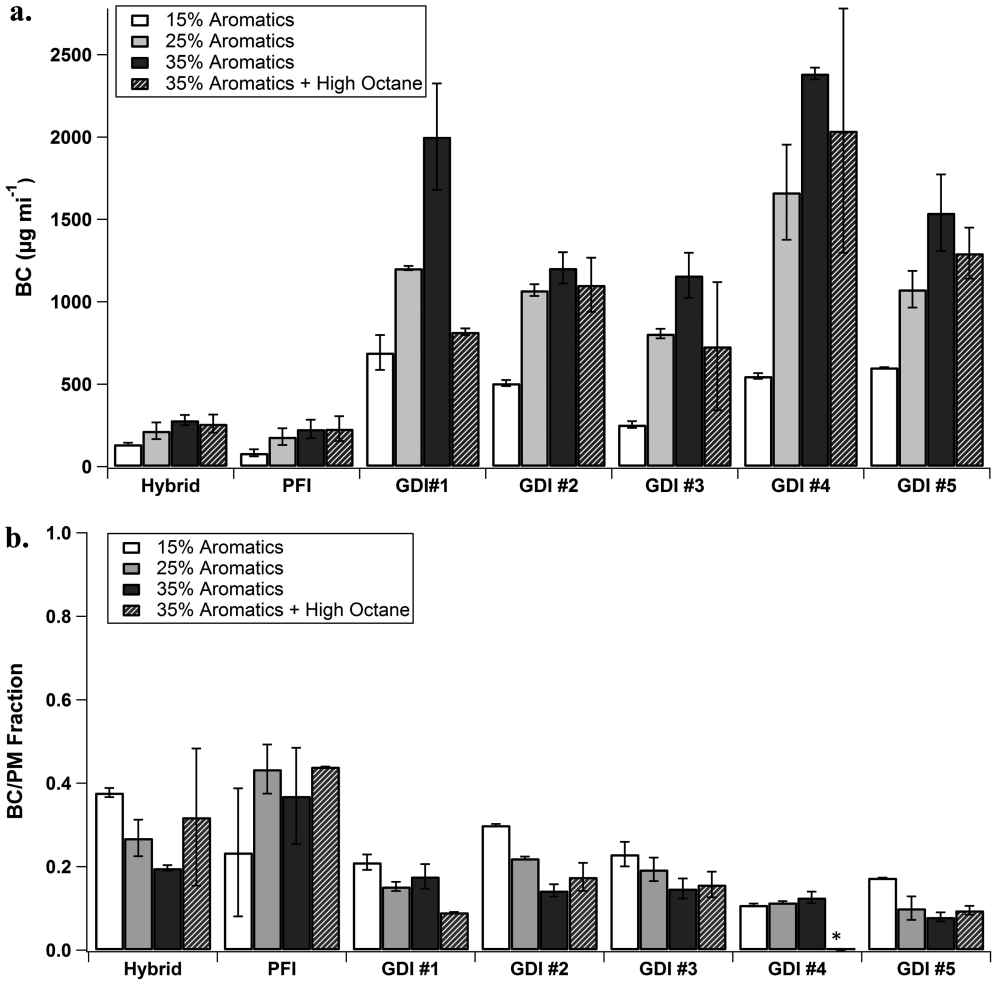

Figure 5. BC emission factor (a.) and BC/PM mass fraction (b.) for all seven vehicles and all fuels driven on the unified cycle (*unavailable data values).

the largest hygroscopicity reduction between the 70 and 50 mph speeds of 73% and the largest κ value for the 70 mph speed of 1.41. This value is exceedingly high, however within 15% uncertainty of reported NaCl values[27] The GDI #1 showed some of the highest κ decreases of all the vehicles in this study with a 91% decrease in the κ values from the 70 to 30 mph speeds for the 35% aromatic fuel with the high octane rating. In addition, the GDI #1 showed a different effect from that of the other vehicles, with large decreases in particle hygroscopicity between the 50 to 30 mph speeds.

BC concentrations are shown in Figure 4b, d, and f. The majority of the trends for all three vehicles show that BC concentration decreases with vehicle speed. This trend was also consistent with particle hygroscopicity. The GDI #2 BC concentration from 70 to 30 mph decreases from 9.445 to 0.340 $\mu g\ m^{-3}$. In addition, BC fuel trends shown during the UC were also seen for the GDI #2 BC concentrations during steady-state speeds. Generally, the BC steady-state fuel trends lacked a consistency compared to the BC EFs over both cycles, which increasing aromatic concentration did not increase the BC concentrations over the steady-state speeds. The BC steady-state concentrations for the GDI #1 followed a relatively similar pattern to those for the UC, where increasing aromatics increased BC emissions.

High vehicle speeds increase particle hygroscopicity and lower particle water-insolubility. Phase 2 of the UC contains higher vehicle speeds and accelerations than the other two phases in the cycle. In addition, steady state vehicle conditions, Figure 4, shows that higher vehicle speeds produce more hygroscopic particles ($\kappa > 1$) compared to lower vehicle speeds ($\kappa < 0.1$). Thus, vehicle speed directly affects particle hygroscopcity. The highest κ value in this study is 1.43 in Figure 4e, which is very similar to the value found for aerosolized NaCl in Short et al.[27] The κ value found in Petters and Kreidenweis[29] for NaCl is 1.28 for CCN derived and 1.33 for growth factor derived values, which comparing 1.43 to both of these are within the 15% uncertainty value associated with this setup. The particles with the highest κ values produced from the vehicles at higher speeds could be inorganic like NaCl or another highly hygroscopic lubrication oil salt, but speciated chemical composition information is required. In general, lubrication oils and vehicle emissions contain very water-soluble salts that could increase the amount of hygroscopic particles.[40−42] Several recent studies have shown that lubrication oil in light-duty vehicles has a major role in the particle emissions composition.[43−45] Thus, at higher speeds the particle emissions could have greater contributions from lubrication oil components. The cumulative WIM fractions reflect emissions at lower vehicle speeds in phase 1 when the majority of the particles are emitted.

3.5. BC Emission Rate. It is assumed that all BC emissions from these vehicles are water-insoluble. The data are the

DOI: 10.1021/acs.est.5b03138
Environ. Sci. Technol. 2015, 49, 10682−10691

weighted average of three trials with the error bars being the standard deviation of those trials. The BC emissions were compared to the WIM fractions by dividing the BC EFs by the total PM mass (shown in the next section). This will be used to determine the BC contribution to the cumulative WIM fraction. Figure 5a shows the BC EFs for all seven vehicles driven over the UC. Increasing aromatic content increases BC EFs. Increased octane rating in fuel reduces the BC EFs for the GDI vehicles. In addition, the GDI vehicles emit more BC and exhibit larger differences in BC with increasing aromatic content compared to the PFI vehicles. The BC EFs for the GDI vehicles ranged from 255 μg mi^{-1} to 2385 μg mi^{-1} with the largest increases were with GDI #3 and GDI #4 by 356% and 334%, respectively, from the 15% to 35% aromatic fuels. The hybrid showed a BC EF increase of 107%, ranging from 136 μg mi^{-1} to 282 μg mi^{1}, between the 15% and 35% aromatic fuels. BC EF for the PFI increased by 175%, ranging from 83 μg mi^{-1} to 228 μg mi^{-1}, between the 15% and 35% aromatic content fuel.

Increased octane rating in fuel reduces the BC EFs for the GDI vehicles. There was no effect from the increase in octane rating for the PFI or hybrid with a BC EF of 230.19 μg m^{-3} and 260.7 μg mi^{-1}, respectively. The increase in octane rating at the 35% aromatic composition had a varying, but definitive, effect for the five GDI vehicles. With the 35% aromatic with high octane fuel, the GDI #1 has a BC emission factor of 817.7 μg mi^{-1}, similar to the 15% aromatic content BC concentration. The higher octane number fuel was similar to the 25% and 35% aromatic content fuel for the GDI #2 vehicle at 1103.1 μg mi^{-1}. The GDI #3 had a BC EF, of 730 μg mi^{-1}, also similar to the 25% aromatic and 35% aromatic BC EF. The BC emissions factor for the 35% aromatic fuel with high octane was 2038.5 μg m^{-3} for the GDI #4 and 1295.6 μg mi^{-1} for the GDI #5. These values were both similar to the 25% and 35% aromatic content BC emissions for their respective vehicles.

BC/PM Mass Fraction. The fraction of BC to PM mass is shown in Figure 5b for all seven vehicles. PM mass emission factors are shown in a companion paper to this study.[24] It should be noted that PM mass measurements were not obtained for the GDI #4 on the 35% aromatic with high octane number fuel. The fractions were averaged for each trial where both PM and BC emission factors were available. The hybrid and PFI vehicles showed larger BC and PM fractions compared to the GDI vehicles. The impact of increasing aromatic content and octane rating was less consistent for the BC to PM fraction than with the BC emission rate. The BC to PM ratios for the hybrid, GDI #2, GDI #3, and the GDI #5 vehicles decreased with increasing aromatic content from 15% to 35%. Interestingly, the hybrid was the only vehicle of this group, which was not a GDI vehicle. The GDI #5 had the largest BC to PM mass fraction decrease, of about 54% between the 15% and 35% aromatic fuels, which was similar to the decrease for the GDI #2 (53%) and the hybrid (48%) vehicles, with the GDI #3 vehicle having the smallest decrease of about 36%. The PFI, GDI #1, and GDI #4 vehicles had statistically similar BC and PM fractions with increasing aromatic content in gasoline. The higher octane rating fuel had similar BC to PM mass fractions to the 35% aromatic content with lower octane rating fuel for the hybrid, PFI, GDI #2, GDI #3, and GDI #5, which were 0.32, 0.44, 0.18, 0.16, and 0.10, respectively. The GDI #1 vehicle showed a significant decrease of 49% in the BC to PM mass fraction for the higher octane number fuel. Overall, the ratios of BC to PM mass were considerably low compared to the overall WIM fractions shown in Figure 3. Over half of all PM emissions are composed of material other than the measured BC in this study. This study is the first to determine the BC EFs, over the UC, from the optical techniques implemented with the MAAP. Other studies have shown measurements of BC using a photoacoustic technique, where the BC contribution to the total PM mass is much larger (~80%).[46−48] However, this study's BC measurements contribute additional information into the complex properties and measurement of BC.

The results showed larger total aromatic concentrations in the fuel increased BC concentrations. However, higher octane ratings in fuels has the potential to reduce BC emissions. BC has the ability to absorb radiative light, thus causing a warming effect.[48−50] If widespread deployment of wall-guided GDI vehicles is to be continued as predicted, then there could be a significant change in climate patterns due to increased amounts of BC. Decreasing the particle emissions from GDI vehicles by changing the fuel, vehicle components used, or by using gasoline particulate filters (GPF) is of the utmost importance. Although the fuels used in this study suggest some fuel components could reduce the PM emissions, more work is needed to determine the chemical components and concentrations in the fuel and lubrication oils that should be reduced. GDI vehicles can emit 5−6 times higher BC compared to the PFI and hybrid vehicles. In addition, the higher aromatic fuels increased the amounts of BC EFs. The 35% aromatic fuel increased the BC EF by as much as 350% from the 15% aromatic fuel. However, BC was reduced with the higher octane rating fuel. If the aromatic content in fuels continues to decrease and higher octane rating fuels become more common (due to higher ethanol blends) then reductions in BC from the higher PM emitting GDI vehicles may occur, but additional research is required to determine the vehicle calibration and configurations role in this trend.

Implications. In the next decade, higher ethanol and lower aromatic content in gasoline may become more common due to the renewable fuels standard (RFS). Our results show that reduced aromatic concentrations are associated with reduced PM mass and (more importantly) reduced BC from GDI vehicles. Thus, increasing the ethanol fraction in gasoline could help to reduce climate and human health impacts attributed to particle emissions from GDI vehicles. Future work should explore the effects of specific aromatic compounds that affect particle emissions whereas this study only correlated results with the total aromatic concentration. As ethanol concentrations are increased in the U.S., the higher octane fuel could effectively decrease BC emissions from the high PM emitting GDI vehicles thus helping to minimize BC.

High vehicular speeds impact the particle hygroscopicity parameter κ and the fraction of water-insoluble particles. This trend was shown during the UC and vehicular stead-state speeds. Water-soluble particles have been shown to have negative effects on human health.[16−18] This is a concern for communities near major freeways where high speeds are typical. In addition, higher vehicle speeds and the increased water-soluble PM emissions found in this study might also have implications on CCN activity.[20] Future studies are needed to elucidate the mechanism connecting vehicles speed/load and the amount of water-insoluble particle emissions. Future work should investigate the fuel and lubricating oil contribution to the particle emissions as the lubricating oil may have a more

DOI: 10.1021/acs.est.5b03138
Environ. Sci. Technol. 2015, 49, 10682−10691

significant contribution to the particle emissions at higher speeds.

■ ASSOCIATED CONTENT

Supporting Information

The Supporting Information is available free of charge on the ACS Publications website at DOI: 10.1021/acs.est.5b03138.

Supplemental Figures S1−S5 and Tables S1 and S2 (PDF)

■ AUTHOR INFORMATION

Corresponding Author

*Phone: (951)-781-5785; e-mail: akua@engr.ucr.edu.

Notes

The authors declare no competing financial interest.

■ ACKNOWLEDGMENTS

We thank Mark Villela and Kurt Bumiller for their technical support on this study. In addition, we thank Tyler Berte, Hans Phang, Chun Liang, and Wartini Ng for their help on the offline measurement analysis. This work was supported by the University of California Transportation Center and the U.S. Environmental Protection Agency (EPA). Diep Vu thanks the U.S. Environmental Protection Agency (EPA) STAR Fellowship Assistance Agreement no. FP-91751101. Specifically, funding for BC measurements were made possible by EPA grant number 83504001. Its contents are solely the responsibility of the grantee and do not necessarily represent the official views of the EPA. Further, the EPA does not endorse the purchase of any commercial products or services mentioned in the publication.

■ REFERENCES

(1) Nadim, F.; Zack, P.; Hoag, G.; Liu, S. United States Experience with Gasoline Additives. *Energy Policy* **2001**, *29* (1), 1−5.

(2) Silva, R.; Cataluna, R.; Weber de Menezes, E.; Samios, D.; Piatnicki, C. M. S. Effect of Additives On the Antiknock Properties and Reid Vapor Pressure of Gasoline. *Fuel* **2005**, *84* (7−8), 951−959.

(3) Perry, R.; Gee, I. L. Vehicle Emissions In Relation to Fuel Composition. *Sci. Total Environ.* **1995**, *169*, 149−156.

(4) The California Reformulated Gasoline Regulations, California Air Resources Board (CARB), Title 13, California Code of Regulations, Section 2261(b).

(5) Weaver, J.; Exum, L.; Prieto, L. *Gasoline Composition Regulations Affecting LUST Sites*, EPA 600/R-10/001. EPA Report. 2010.

(6) U.S. Environmental Protection Agency. *Fuels and fuel additives, renewable fuel standard*. http://www.epa.gov/otaq/fuels/renewablefuels.

(7) EPA. *Draft Regulatory Impact Analysis: Tier 3 Motor Vehicle Emission and Fuel Standards*, EPA-420-D-13-002; U.S. Environmental Protection Agency, 2013.

(8) Zhao, F.; Lai, M. C.; Harrington, D. L. Automotive Spark-Ignited Direct-Injection Gasoline Engines. *Prog. Energy Combust. Sci.* **1999**, *25* (5), 437−562.

(9) Graham, L. Chemical Characterization of Emissions From Advance Technology Light- Duty Vehicles. *Atmos. Environ.* **2005**, *39* (13), 2385−2398.

(10) Liang, B.; Ge, Y.; Tan, J.; Han, X.; Gao, L.; Hao, L.; Ye, W.; Dai, P. Comparison of PM Emissions From a Gasoline Direct Injected (GDI) vehicle and a Port Fuel Injected (PFI) vehicles measured by Electrical Low Pressure Impactor (ELPI) With Two Fuels: Gasoline and M15 Methanol Gasoline. *J. Aerosol Sci.* **2013**, *57*, 22−31.

(11) Piock, W.; Hoffmann, G.; Berndorfer, A.; Salemi, P.; Fusshoeller, B. Strategies towards meeting future particulate matter emission requirements in homogeneous gasoline direct injection engines. *SAE Int. J. Engines* **2011**, *4*, 1455−1468.

(12) Ramgolam, K.; Favez, O.; Cachier, H.; Gaudichet, A.; Marano, F.; Martinon, L.; and Baeza-Squiban, A. Size-partitioning of an urban aerosol to identify particle determinants involved in the proinflammatory response induced in airway epithelial cells. *Part. Fibre Toxicol.*. **2009**, *6*(10).1010.1186/1743-8977-6-10

(13) Gutiérrez-Castillo, M.; Roubicek, D. A.; Cebrián-Garcia, M. E.; De Vizcaya-Ruiz, A.; Sordo-Cedeòo, M.; Ostrosky-Wegman, P. Effect of chemical composition on the induction of DNA damage by urban airborne particulate matter. *Environ. Mol. Mutagen.* **2006**, *47*, 199−211.

(14) Valavandidis, A.; Fiotakis, K.; Vlachogianni, T. Airborne Particulate Matter and Human Health: Toxicological Assessment and Importance of Size and Composition of Particles for Oxidative Damage and Carcinogenic Mechanisms. *Journal of Environmental Science and Health, Part C* **2008**, *26* (4), 339−362.

(15) Squires, P. The microstructure and colloidal stability of warm clouds. *Tellus* **1958**, *10* (2), 256−261.

(16) Geller, M. D.; Ntziachristos, L.; Mamakos, A.; Samaras, Z.; Schmitz, D. A.; Fraines, J. R.; Sioutas, C. Physicochemical and redox characteristics of particulate matter (PM) emitted from gasoline and diesel passenger cars. *Atmos. Environ.* **2006**, *40* (36), 6988−7004.

(17) Verma, V.; Shafer, M. M.; Schauer, J. J.; Sioutas, C. Contribution of Transistion Metals In the Reactive Oxygen Species Activity of PM Emissions From Retrofitted Heavy-Duty Vehicles. *Atmos. Environ.* **2010**, *44* (39), 5165−5173.

(18) Biswas, S.; Verma, V.; Schauer, J. J.; Sioutas, C. Chemical Speciation of PM Emissions From Heavy-Duty Diesel Vehicles Equipped With Diesel Particulate Filter (DPF) and Selective Catalytic Reduction (SCR) Retrofits. *Atmos. Environ.* **2009**, *43*, 1917−1925.

(19) Longest, P. W.; McLeskey, J. T.; Hindle, M. Characterization of Nanoaerosol Size Change During Enhanced Condensational Growth. *Aerosol Sci. Technol.* **2010**, *44* (6), 473−483.

(20) Ervens, B.; Feingold, G.; Kreidenweis, S.M. Influence of water-soluble organic carbon on cloud drop number concentration. *J. Geophys. Res.* **2005**, *110*, D18211.

(21) Storey, J. M.; Barone, T.; Norman, K.; Lewis, S. Ethanol Blend Effects on Direct Injection Spark-Ignition Gasoline Vehicle Particulate Matter Emissions. *SAE Technical Paper* **2010**, *3*, 2010−01−2129.

(22) Maricq, M. M.; Szente, J. J.; Jahr, K. The Impact of Ethanol Fuel Blends on PM Emissions from a Light-Duty GDI Vehicle. *Aerosol Sci. Technol.* **2012**, *46* (5), 576−583.

(23) Chen, L.; Stone, R.; Richardson, D. A Study of Mixture Preparation and PM Emissions Using a Direct Injection Engine Fuelled with Stoichiometric Gasoline/Ethanol Blends. *Fuel* **2011**, *96*, 120−130.

(24) Karavalakis, G.; Short, D.; Vu, D.; Russell, R.; Hajbabaei, M.; Asa-Awuku, A.; Durbin, T. Evaluating the Effect of Aromatics in Gasoline on Gaseous and Particulate Matter Emissions From SI-PFI and SI-DI Vehicles. *Environ. Sci. Technol.* **2015**, *49* (11), 7021−7031.

(25) Wang, S. C.; Flagan, R. C. Scanning Electrical Mobility Spectrometer. *Aerosol Sci. Technol.* **1990**, *13*, 230−240.

(26) Short, D.; Giordano, M.; Zhu, Y.; Fine, P.; Polidori, A.; Asa-Awuku, A. A Unique On-line method to infer black carbon contributions to water-insoluble contributions. *Aerosol Sci. Technol.* **2014**, *48* (7), 706−714.

(27) Short, D.; Vu, D.; Durbin, T. D.; Karavalakis, G.; Asa-Awuku, A. Particle Speciation of Emissions from Iso-butanol and Ethanol Blended Gasoline in Light-Duty Vehicles. *J. Aerosol Sci.* **2015**, *84*, 39−52.

(28) Hering, S. V.; Stolzenburg, M. R. A Method for Particle Size Amplification by Water Condensation in a Laminar, Thermally Diffusive Flow. *Aerosol Sci. Technol.* **2005**, *39*, 428−436.

(29) Petters, M. D.; Kreidenweis, S. M. A single parameter representation of hygroscopic growth and cloud condensation nucleus activity. *Atmos. Chem. Phys.* **2007**, *7*, 1961−1971.

(30) Turpin, B. J.; Lim, H. Species Contributions to PM 2.5 Mass Concentrations: Revisiting Common Assumptions for Estimating Organic Mass. *Aerosol Sci. Technol.* **2001**, *35* (1), 602−610.

(31) Schwarz, J. P.; Gao, R. S.; Fahey, D. W.; Thomson, D. S.; Watts, L. A.; Wilson, J. C.; Reeves, J. M.; Darbeheshti, M.; Baumgardner, D. G.; Kok, G. L.; Chung, S. H.; Schulz, M.; Hendricks, J.; Lauer, A.; Kärcher, B.; Slowik, J. G.; Rosenlof, K. H.; Thompson, T. L.; Langford, A. O.; Loewenstein, M.; Aikin, K. C. Single-particle measurements of midlatitude black carbon and light-scattering aerosols from the boundary layer to the lower stratosphere. *J. Geophys. Res.* **2006**, *111*, D16207.

(32) Chueng, K. L.; Polidori, A.; Ntziachristos, L.; Tzamkiozis, T.; Samaras, Z.; Cassee, F. R.; Gerlofs, M.; Siouras, C. Chemical Characteristics and Oxidative Potential of Particulate Matter Emissions from Gasoline, Diesel, and Biodiesel Cars. Environ. *Environ. Sci. Technol.* **2009**, *43*, 6334−6340.

(33) Yung-Fang, Y. Y. Oxidation of alkanes over noble metal catalysts. *Ind. Eng. Chem. Prod. Res. Dev.* **1980**, *19*, 293−298.

(34) Canvani, F.; Trifiró, F. Selective oxidation of light alkanes: interation between the catalyst and the gas phase on different classes of catalytic materials. *Catal. Today* **1999**, *51* (3−4), 561−580.

(35) Curran, H. J.; Gaffuri, P.; Pitz, W. J.; Westbrook, C. K. A comprehensive modeling study of iso-octane oxidation. *Combust. Flame* **2002**, *129* (3), 253−280.

(36) Ervens, B.; Feingold, G.; Kreidenweis, S. M. Influence of water-soluble organic carbon on cloud drop number concentration. *J. Geophys. Res.* **2005**, *110*, D18211.

(37) Ekman, A. M. L.; Engstrom, A.; Wang, C. The effect of aerosol composition and concentration on the development and anvil properties of a continental deep convective cloud. *Q. J. R. Meteorol. Soc.* **2007**, *133*, 1439−1452.

(38) Pierce, J. R.; Adams, P. J. Uncertainty in global CCN concentrations from the uncertain aerosol nucleation and primary emissions rates. *Atmos. Chem. Phys.* **2009**, *9*, 1339−1356.

(39) Shantz, N. D.; Leaitch, W. R.; Phinney, L.; Mozurkewich, M.; Toom-Sauntry, D. The effect of organic compounds on the growth rate of cloud droplets in marine and forest settings. *Atmos. Chem. Phys.* **2008**, *8*, 5869−5887.

(40) Uy, D.; Ford, M. A.; Jayne, D. T.; O'Neill, A. E.; Haack, L. P.; Hangas, J.; Jegner, M. J.; Sammut, A.; Gengopadhyay, A. K. Characterization of gasoline soot and comparison to diesel soot: Morphology, chemistry, and wear. *Tribol. Int.* **2014**, *80*, 198−209.

(41) Cheng, Y.; Lee, S. C.; Ho, K. F.; Chow, J. C.; Watson, J. G.; Louie, P. K. K.; Cao, J. J.; Hai, X. *Science of the Total Environment* **2009**, *408* (7), 1621−1627.

(42) Cheung, K. L.; Ntziachristos, L.; Tzamkiozis, T.; Schauer, J. J.; Samaras, Z.; Moore, K. F.; Sioutas, C. Emissions of particulate trace elements, metals, and organic species from Gasoline, Diesel, and Biodiesel passenger vehicles and their relation to oxidative potential. *Aerosol Sci. Technol.* **2010**, *44*, 500−513.

(43) Sonntag, D. B.; Bailey, C. R.; Fulper, C. R.; Baldauf, R. W. Contribution of Lubricating Oil to Particlae Matter Emissions from Ligh-Duty Gasoline Vehicles in Kansas City. *Environ. Sci. Technol.* **2012**, *46*, 4191−4199.

(44) Worton, D. R.; Isaacman, G.; Genter, D. R.; Dallmann, T. R.; Chan, A. W. H.; Ruehl, C.; Kirchstetter, T. W.; Wilson, K. R.; Harley, R. A.; Goldstein, A. H. Lubricating Oil Dominates Primary Organic Aerosol Emissions from Motor Vehicles. *Environ. Sci. Technol.* **2014**, *48*, 3698−3706.

(45) Kleeman, M. J.; Riddle, S. G.; Robert, M. A.; Jakober, C. A. Lubricating Oil and Fuel Contributions to Particulate Matter Emissions From Light-Duty Gasoline and Heavy-Duty Diesel Vehicles. *Environ. Sci. Technol.* **2008**, *42* (1), 235−242.

(46) Storey, J. M.; Lewis, S.; Szybist, J.; Thomas, J.; Barone, T.; Eibl, M.; Nafziger, E.; Kaul, B. Novel characterization of GDI engine exhaust for gasoline and mid-level gasoline-alcohol blends. *SAE Technical Paper* **2014**, *7*, 2014−01−1606.

(47) Khalek, I. A.; Bougher, T.; Jetter, J. J. Particle emissions from a 2009 gasoline direct injection engine using different commercially available fuels. *SAE Int. J. Fuels Lubr.* **2010**, *3* (2), 623−637.

(48) Maricq, M. M.; Szente, J. J.; Adams, J.; Tennison, P.; Tumpsa, T. Influence of mileage accumulation on the paticle mass and number emissions of two gasoline direct injection vehicles. Environ. *Environ. Sci. Technol.* **2013**, *47* (20), 11890−11896.

(49) Bond, T. C.; Doherty, S. J.; Fahey, D. W.; Forster, P. M.; Berntsen, T.; DeAngelo, B. J.; Flanner, M. G.; Ghan, S.; Karcher, B.; Koch, D.; Kinne, S.; Kondo, Y.; Quinn, P. K.; Sarofim, M. C.; Schultz, M.; Venkataraman, C.; Zhang, H.; Zhang, S.; Bellouin, N.; Guittikunda, S. K.; Hopke, P. K.; Jacobson, M. Z.; Kaiser, J. W.; Klimont, Z.; Lohmann, U.; Schwarz, J. P.; Shindell, D.; Storelvmo, T.; Warren, S. G.; Zender, C. S. Bounding the Role of Black Carbon in the Climate System: A Scientific Assessment. *Jounral of Geophysical Research: Atmospheres* **2013**, *118*, 5380−5552.

(50) Ramanathan, V.; Carmichael, G. Global and Regional Climate Changes Due to Black Carbon. *Nat. Geosci.* **2008**, *1*, 221−227.

DOI: 10.1021/acs.est.5b03138
Environ. Sci. Technol. 2015, 49, 10682−10691